

Astroparticle Physics

Norbert Magnussen

Fachbereich Physik, Universität Wuppertal, D-42097 Wuppertal, Germany
E-mail: magnus@wpos7.physik.uni-wuppertal.de

Abstract

This article† reviews some recent developments in Astroparticle Physics. Due to the extension of the field only part of the results and developments can be covered. The status of the search for Dark Matter, some recent results on Cosmic Rays and Gamma Ray Astronomy and the status of Neutrino Astronomy are presented.

1. Introduction

Astroparticle Physics is rapidly growing into a diversified field of observational and phenomenological physics, addressing questions ranging from the nature and distribution of Dark Matter, the mass of neutrinos and the origin of the Cosmic Rays, to the existence of antimatter. In addition the level and source composition of cosmologically important extragalactic diffuse radiation levels are probed and tests are performed on non-Lorentz invariant interaction and propagation terms predicted, e.g., in several ansätze for Quantum Gravity theories.

Among the results and developments not covered here are the latest developments in gravitational wave antennas (for a recent review see, e.g., [1]), the results on atmospheric neutrinos (see [2]), the measurements of the Cosmic Rays composition and spectra around the 'knee' in the all-particle spectrum (see, e.g., [3]), or the results from the first flight of the AMS detector [4].

The structure of this paper is as follows: section 2 reviews the status of the Dark Matter search. The importance of Cosmic Ray measurements at low and high energies are discussed in section 3 followed by some of the latest developments in Gamma and Neutrino Astronomy in sections 4 and 5, respectively. A brief outlook is given in section 6.

2. The Dark Problems

Some recent reviews on cosmology, e.g., [5], conclude that for the first time now we have a *complete* observational accounting of matter and energy in the Universe consistent with Λ CDM (i.e., Cold Dark Matter plus non-zero Λ term)

inflationary cosmology. This, however, is not equivalent to a complete understanding of these ingredients, and according to one summary shown in figure 1 the three *Dark Problems* that we are facing today are: Where are the dark baryons? What is the non-baryonic Dark Matter? What is the Dark Energy recently detected in analyses of distant supernovae [6, 7]? In the following the status of the questions concerning the amount and nature of Dark Matter (DM) will be addressed.

The evidence for DM is manifold and can roughly be divided into evidence on galactic scales (i.e., $\mathcal{O}(10)$ kpc) and on galaxy cluster scales (i.e., $\mathcal{O}(10)$ Mpc). Measurements of rotation curves of galaxies [8], especially of spiral galaxies including the Milky Way, still give the most convincing evidence for the presence of a galactic Dark Matter (DM) mass component which is about a factor 10 larger than the observed luminous matter. Most of this mass has to be distributed in an extended halo in an approximately spherical distribution with density falling as $1/r^2$. Inspection of figure 1 shows that this factor can in principle be accommodated by baryons produced in Big Bang Nucleosynthesis (BBN). On scales of the extension of rich galaxy clusters the second DM problem becomes visible. The main mass fraction of rich clusters is in form of hot intracluster gas, the mass of which can be inferred by measuring the X-ray flux or by mapping the Sunyaev-Zel'dovich decrement caused by the scattering of cosmic microwave background (CMB) photons on the hot electrons. The total cluster mass is then derived by one or more of three methods: from motion of the galaxies utilizing the virial theorem, by assuming hydrostatic equilibrium for the hot gas, or, in some cases, by gravitational lensing. From these data the mean matter density in the Universe, Ω_M , can be inferred. The obtained value of $\Omega_M = 0.4 \pm 0.1$ is consistent with values derived from other observables like bulk matter

† Invited review at EPS-HEP '99, July 1999, Tampere, Finland.

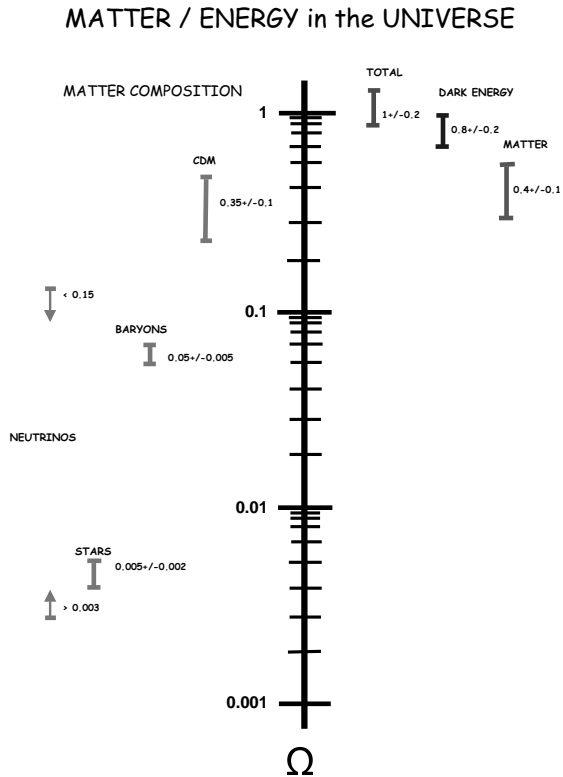


Figure 1. Current status of the observational and theoretical census of matter and energy in the Universe. From [5].

flow or the peculiar motion of our Local Group of galaxies (e.g., [5]). Assuming BBN to be correct the main matter component in the Universe thus has to be *non-baryonic*. Note that the validity of BBN is well tested by the measured ^4He , D, ^3He , and ^7Li abundances (e.g., [9]). In addition to the data there are solid theoretical arguments for the existence of a large non-baryonic DM mass fraction in the Universe. E.g., without large amounts of non-baryonic DM there is no working theory of galaxy formation consistent with the small level of fluctuations observed in the CMB.

So far DM has only been discovered by its gravitational effects and the search for the manifestation of DM in other interactions mainly is limited to searches for galactic DM. These searches can either focus on the baryonic or a possible non-baryonic component. Note that a debate on whether any non-baryonic component is present at galactic scales at all has been going on since the first solid evidence for galactic DM was obtained.

2.1. Search for Baryonic Dark Matter

Candidates for the baryonic component are low mass stars, stellar remnants, Massive Astrophysical Compact Halo Objects (MACHOs) such as brown dwarfs and Jupiters with masses below $\sim 0.09 M_{\odot}$, cold molecular clouds, or very massive black holes. Of these candidates all but the cold molecular clouds are in principle detectable by *gravitational microlensing*.

Gravitational microlensing (ML) as a means to search for MACHOs was proposed in a seminal paper by Paczyński [10] in 1986. Only 13 years after this proposal ML is a thriving field and can be considered a new field of *galactic astronomy* (for a review see, e.g., [11]). Several different target directions have been monitored in the search for the transient ML events characterized by the achromatic, symmetric and unique amplification of a source star. The pioneering work was performed by the EROS and MACHO collaborations who in the last years monitored millions of stars in the small (SMC) and large (LMC) Magellanic Clouds (see figure 2) and announced the first candidate events in 1993 [12, 13]. The total ML events statistics towards the SMC and LMC currently is about 20 events (from EROS, MACHO, and OGLE). Other target directions have been the galactic bulge (e.g., OGLE, OGLE-2, DUO, MOA, and MACHO), galactic spiral arms (e.g., EROS), or towards the Andromeda galaxy (AGAPE). In addition new collaborations (e.g., MACHO/GMAN, MPS, or PLANET) aim at accurate photometry of ML events in order to search for planets in the source star systems. The ML event statistics towards galactic targets is currently more than 400 and is utilized to study details of galactic structure unobservable by other methods (see, e.g., [14]).

For the interpretation of ML events in terms of DM one has to take into consideration that the velocity, distance and MACHO mass degeneracy in the basic ML equations (see Eq. (1) and (2)) does not allow to determine the location of the lenses itself based on the magnification and duration of the event alone. Only for special events like binary ML events discovered towards the Magellanic clouds and long duration events showing parallax effects due to the movement of the earth around the sun is it possible to constrain the location of the lenses. E.g., for the binary-lens caustic crossing event MACHO-98-SMC-1 which was monitored by 5 ML collaborations after the MACHO alert, the combined analysis yields strong evidence for the lens system to be located in the SMC itself [15].

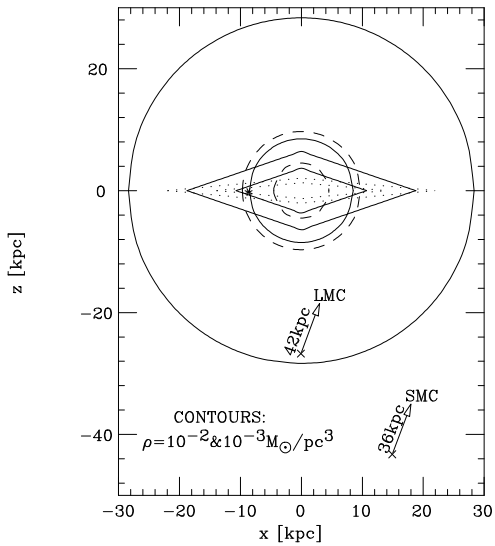


Figure 2. Schematic view of lensing populations discussed for the Galaxy: the standard spherical halo (solid lines), a heavy spheroid (dashed lines), a maximum thick disk (solid lines) and a dark thin disk (dotted lines). For each population the density contours $\rho = 10^{-3}$ and $\rho = 10^{-2} M_{\odot}/\text{pc}^3$ are shown. The locations of the sun and the small (SMC) and large (LMC) Magellanic Clouds are indicated. From [11].

In general, however, the basic ML equations only relate the velocity, distance and mass of the lenses to give the lensing probability:

$$\tau \propto \int \rho(x)x(1-x)dx \quad (1)$$

with the mass density distribution, $\rho(x)$, of microlensing matter needed as an input according to the adopted *isotropic halo model* (see figure 2), and $x = D_{\text{lens}}/D_{\text{source}}$ with D_{lens} and D_{source} the distances of the lens and the source star, respectively. The duration of the lensing event is given by:

$$\Delta t \propto \sqrt{\frac{Mx(1-x)}{v_{\perp}^2}} \quad (2)$$

with M the mass and v_{\perp} the transverse velocity of the lens. The lensing probability, τ , gives the probability for finding a source star within the Einstein radius, R_E , of some MACHO and which thus is magnified by a factor $A = 1.34$. The smallness of τ ($\mathcal{O}(10^{-6})$) makes it necessary to simultaneously monitor millions of stars.

The combined limits and results on the galactic halo mass fraction in form of MACHOs from the

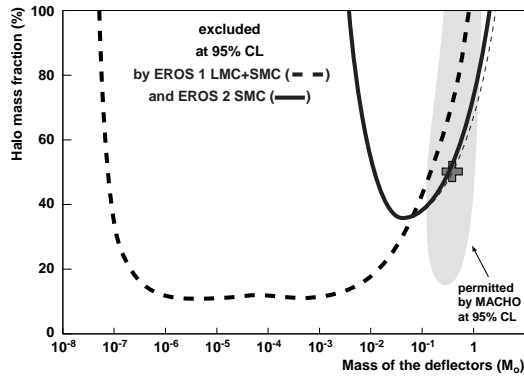


Figure 3. Exclusion diagram at 95% CL assuming the standard spherical halo. The dashed line is the limit from EROS 1 towards the LMC and SMC [17], the solid line is the limit from EROS 2 towards the SMC [16]. The 95% CL allowed region from the MACHO collaboration is shown as the shaded area [18] with the preferred value indicated by the cross. The thin dashed line corresponds to the limit obtained under the assumption that no halo event has been observed. From [16].

observations of the LMC and SMC by the EROS and MACHO collaborations are shown in figure 3 [16]. From the lack of short duration events it can be concluded that MACHOs in the mass range $10^{-7} M_{\odot} \lesssim m \lesssim 10^{-3} M_{\odot}$ make up less than 25% of the halo mass for most halo models. On the other hand, the MACHO collaboration derived a most probable MACHO mass range of $m = 0.5^{+0.3}_{-0.2} M_{\odot}$ from the observation of the average long duration of 8 candidate ML events in the first 2.1 years of LMC data [18]. In addition this event rate is compatible with about 50% of the mass of the halo in the form of MACHOs of this mass. In figure 3 the 95% CL allowed halo mass fraction region as a function of m_{MACHO} derived from these data is also shown. Recently the EROS collaboration published its results on the first 2 years of observation towards the SMC [16]. Only one ML candidate event was observed. This low event rate can be transformed into a limit on the fraction of the halo made out of heavy MACHOs assuming a standard spherical halo model. The 95% CL exclusion limit is shown as the heavy solid line in figure 3 and now excludes a halo completely made out of heavy (i.e., $\sim 0.5 M_{\odot}$) MACHOs. Note that these limits are lower if some of the observed ML events are due to self-lensing. Self-lensing means that the lenses are not in the halo but in tidally elongated Magellanic clouds themselves or in the (warped) disk of our own galaxy. In addition the lensing events might be due to faint stars of an yet undiscovered intervening

dwarf galaxy. If the ML events should be caused by one of the above effects MACHOs will be irrelevant for DM whatever their astrophysical nature. In order to study this further and get a better handle on the location of the lenses through the comparison of mass moments extracted from the ML data with halo models (e.g., [11]) a much larger event statistics towards the LMC and SMC and other line-of-sights are necessary.

Independent constraints on the DM contribution of baryonic compact objects come from astrophysics and cosmology which now rule out most of the compact candidates for baryonic DM in the halo. Without discussing each limit in detail the situation of protostellar objects, stellar objects and stellar remnants as candidate objects for making up the halo mass can be summarized as follows:

- Jupiters ($10^{-7} < M < 10^{-2} M_{\odot}$) are ruled out by ML data, i.e., halo mass fraction $< 25\%$.
- faint hydrogen burning stars ($M > 0.09 M_{\odot}$) and young brown dwarfs ($M < 0.09 M_{\odot}$) are ruled out on the basis of HST and ISO data and contribute a halo mass fraction of $\lesssim 0.01$ [19].
- old brown dwarfs ($M < 0.09 M_{\odot}$) are ruled out by HST and US Naval Observatory parallax data and star formation theory and contribute a fraction $\lesssim 0.03$ [20].
- white dwarfs (wd), neutron stars, and black hole stellar remnants are ruled out by observations strongly constraining the number of possible progenitor stars. The constraining data range from chemical abundances of C and N measured in Ly α systems [21], global D and ^4He abundances [22], to the stringent limit on the cosmic infrared background flux inferred from the observation of multi-TeV γ -rays from the blazar Mrk 501 at a redshift of $z = 0.034$ [23]. All of these signal levels would have been raised by progenitor stars, yielding:

$$\begin{aligned} - \Omega_{wd} h &\leq 2 \times 10^{-4} \text{ [21]} \\ - \Omega_{wd} h &< 0.003 \text{ [22]} \\ - \Omega_{wd} h &\leq (1-3) \times 10^{-3} \text{ [24]} \end{aligned}$$

with the Hubble parameter $H_0 = h \cdot 100 \text{ km s}^{-1} \text{ Mpc}^{-1}$.

In conclusion, the ML data in combination with current astrophysics seem to rule out a completely baryonic halo, *if* it is made out of isotropically distributed compact massive objects. The nature of the observed events towards the LMC and SMC remains unknown. One possible explanation is a halo made out of *primordial* black holes with a mass of about one solar mass which would explain the ML events and act as cold DM otherwise. Other exotic

candidates like mirror matter stars which would also circumvent the astrophysical limits are discussed in the literature (e.g., [27]). An astrophysics scenario which would still allow for a purely baryonic halo is a halo made out of cold molecular clouds (see, e.g., [25]) without explaining the ML events. However, most of the data and theoretical models currently point to a substantial fraction of the halo being made up by non-baryonic DM.

2.2. Search for Non-Baryonic Dark Matter

Experiments have to answer the question of the nature of the non-baryonic DM (NBDM). The search for observable signals resulting from interactions other than gravity in general require detectors especially suited to the DM candidate in question.

At the moment there is a surplus of matter (types) in cosmology and at the same time important stable and massive particles predicted to exist either within the Standard Model or in its plausible extensions have not yet been discovered. The most promising approach to searches for NBDM therefore lies in performing dedicated searches for selected Particle Physics candidates. These have to fulfill the requirement to have decoupled from the primeval plasma when their interaction rate became smaller than the cosmic expansion rate and which therefore would be floating around the Universe today as *relic particles*. According to their energies at the time of decoupling one differentiates between relativistic (for masses less than 1 keV), i.e., hot, and non-relativistic, i.e., cold, relics. The best candidates which could contribute significantly to the mass-energy density in the Universe (i.e., $\Omega \sim 1$) are the axion, the neutrino, the lightest supersymmetric particle if R-parity is conserved, or magnetic monopoles. Note that monopoles do not work well in numerical simulations of structure formation and are thus regarded to be the least probable solution to the NBDM problem by most cosmologists and we shall in the following not discuss experimental searches for monopoles.

Of the remaining candidates the axion is a very good candidate but hard to detect in laboratory experiments within the current mass constraints. It is the Goldstone boson of the U(1) Peccei-Quinn symmetry [28] as the elegant solution to the strong CP problem of QCD. At the same time it would be a good cold DM (CDM) candidate as, within the current laboratory and cosmological limits, relic axions could make up a significant fraction of the critical density. The sensitivity of experiments searching for light axions via the

Primakoff conversion of axions into microwave photons in strong magnetic fields are now entering into the cosmological interesting range [29]. See [30] for a detailed review of the recent development and the current limits which mainly stem from astrophysics and cosmology

The next candidate, a light massive neutrino, would be a hot DM (HDM) particle and its mass would be directly proportional to its contribution to Ω . More precisely, the sum of the mass eigenstates which contribute to the active flavour neutrinos is directly proportional to Ω_ν . In order for the structure formation theories to work neutrinos (or other HDM) cannot be responsible for the whole non-baryonic DM fraction but have to give a contribution to Ω of $\lesssim 0.15$. This can be translated into $\sum M_i \lesssim 6$ eV (for $H_0 = 65 \text{ km} \cdot \text{s}^{-1} \cdot \text{Mpc}^{-1}$ and $i = 1, \dots, 3$) [5]. This number, derived from a cosmological measurement, i.e., the fluctuation spectrum of the cosmic microwave background, is compatible with (and competitive to) the direct determination of the mass of the electron antineutrino in the measurement of the endpoint of the β spectrum in tritium decay. These experiments now start to consistently yield a positive antineutrino mass in the fit, with the current value from the Mainz experiment reported at this conference of $m_{\bar{\nu}} \leq 2.8$ eV (95% CL) [31]. In spite of the large relic neutrino density (54 cm^{-3} per light flavour) the determination of their exact contribution to Ω will most probably come from this type of direct laboratory experiments, 2β decay experiments (e.g., [32]), or the forthcoming long-baseline oscillation experiments (e.g., [2]). However, as the 2β decay experiments only give a mass convolution involving unknown phases and oscillation experiments only give mass differences, the improvement of the cosmological limits will continue to be important.

The fundamental questions that are left open by the Standard Hot Big Bang Cosmology point towards a grander theory. The best candidate to date is Inflation plus cold Dark Matter leading to a flat and slowly moving Universe. In addition Particle Physics models beyond the Standard Model offer a variety of CDM candidate particles. As Superstring theories predict a Supersymmetry sector at the TeV scale the favourite CDM candidate in extensions of the Standard Model is the Lightest Supersymmetric Particle (LSP), presumably the neutralino, in minimal supersymmetric models with conserved R-parity. If these particles have been produced in the early Universe and have decoupled when they became non-relativistic their density would be inversely proportional to their interaction rate.

The requirement that the LSP contributes to Ω of $\mathcal{O}(1)$ makes it weakly interacting with a mass between ~ 10 GeV and ~ 500 GeV [33], hence Weakly Interacting Massive Particle (WIMP).

Assuming that WIMPs contribute a substantial fraction to the galactic halo mass leads to a density at the location of the earth in the range of $0.3 - 0.4 \text{ GeV cm}^{-3}$ in the isothermal standard halo picture (depending slightly on the chosen halo parameters). WIMPs can be detected directly or indirectly, where their elastic scattering on matter constitutes the direct channel and the detection of annihilation products expected from pairwise annihilation processes define the indirect channels.

The direct searches are based on the detection of nuclear recoils of $\mathcal{O}(\text{keV})$ as signals of the elastic scattering process within the sensitive detector volume. The expected signal distribution is roughly exponential with the mean depending on the mass of the WIMP. The expected signals rates are of the order of 1 event per day and kg of detector mass. In the scattering only a small fraction of the delivered energy, however, goes into the ionization channel. Most of the energy is released as heat and cryogenic devices are therefore intensely studied for their suitability. The main background is due to electron recoils from Compton scattering of background γ -rays. Due to the motion of the earth through the WIMP halo an annual modulation of the direct scattering signal with an amplitude of the order of a few % is expected.

Detectors with a low inherent radioactive background like Germanium, NaI, or cryogenic detectors are mostly used to search for WIMP scattering signals (e.g., [34] for a review). The DAMA collaboration presented a hint for an annual modulation signal in 1997 [35] and recently announced $\sim 3\sigma$ evidence for annual modulation after quadrupling the analysed statistics [36]. The residual detector count rate versus time is shown in figure 4. The 90% CL allowed region of scalar WIMP-nucleon scattering cross section versus WIMP mass only barely enters into the region expected in constrained minimal supersymmetric models (CMSSM) (see figure 5). The constrained or 'phenomenological' MSSM is the simplest supersymmetric extension of the Standard Model with the number of free parameters of the most general R-parity conserving model of 124 reduced to 7 real parameters. Two other NaI experiments, the UK Dark Matter Collaboration (UKDMC) [40] which is taking data since 1996 in the UK Boulby Mine and a French experiment at Modane [41] studying NaI(Tl) crystals for their suitability as DM detectors, use the PMT pulse shapes to identify and distinguish against α , β ,

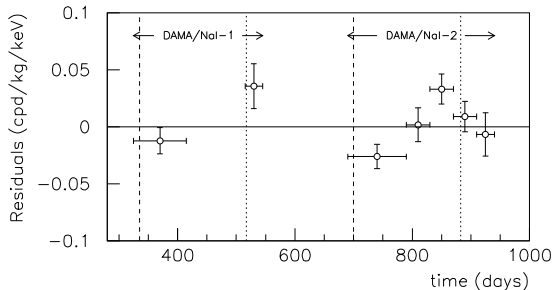


Figure 4. Residual count rate versus time elapsed since January 1 of the first year of DAMA data taking. The expected modulation is a cosine function with minimum at December 2 and the maximum at June 2. From [37].

and γ backgrounds. Both experiments find a not yet understood population of short pulses not consistent with background expectation according to elaborate background studies (e.g., [42]). These data are also not fully compatible to the WIMP signal expectation and are thus not interpreted in terms of a WIMP signal. Due to the poor intrinsic background rejection capability of NaI detectors rather some hidden systematics is suspected. In order to test the DAMA evidence in future searches the active identification of the background will be of foremost importance (e.g., with liquid Xenon or cryogenic devices). Note that, e.g., the current UKDMC sensitivity is comparable to DAMA. Some of the existing limits on the scalar WIMP-nucleon cross section versus WIMP mass together with some expected sensitivities for some of the planned experiments are shown in figure 5.

Indirect searches for WIMP DM are based on the detection of the products of pairwise WIMP annihilation in the galactic halo or in the centre of earth or sun. This process will occur if the WIMP is the supersymmetric neutralino, χ , i.e., a Majorana fermion. One of its characteristics is the production of equal amounts of matter and antimatter and all stable annihilation products, e.g., p , \bar{p} , e^- , e^+ , \bar{D} , ν , may serve as signature. In addition γ s can be produced in loop-induced annihilation reactions [44, 45]. Whereas protons and electrons are too abundant in the normal Cosmic Rays, antimatter, which does not exist in sizable quantities in the observable Universe, may herald the annihilation of neutralinos in the galactic halo. The expected annihilation rate depends on the WIMP density distribution in the halo. According to the halo models shown in figure 2 and according to results of N-body simulations of the formation of dark halos

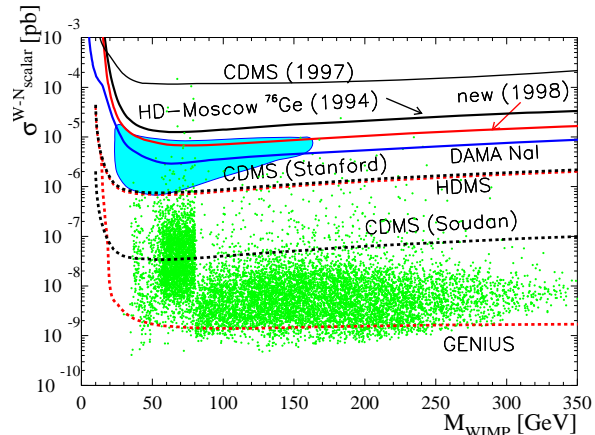


Figure 5. WIMP-nucleon cross section limits for scalar interactions as a function of WIMP mass. The shaded area indicates the DAMA 90% CL evidence contour. The solid lines indicate excluded regions. The broken lines indicate the expected sensitivity for the ongoing CDMS experiment at different sites [39] and the proposed GENIUS experiment [43]. See [38] for full references. From [38].

a considerable enhancement of the DM density near the Galactic centre (GC) is expected. For the $\chi\chi \rightarrow \gamma X_0$ channel this will lead to a much enhanced signal from the direction of the GC where X_0 is a neutral particle of mass m_{X_0} and the γ 's will be nearly monochromatic with an energy

$$E_\gamma = M_\chi - \frac{m_{X_0}^2}{4M_\chi}.$$

Due to the non-relativistic velocities of the WIMPs this channel thus is characterized by a huge signal peak-to-width ratio with no known astrophysical background source. The proposal to use ground-based Imaging Air Cherenkov Telescopes (IACTs) to search for this signal dates back to 1992 [46] when it was realized that the only average energy resolution of the order of 10-20% is offset by the huge collection areas of the order of 10^4 - 10^6 m². According to recent calculations [47] the upcoming generation of IACTs (see section 4) will provide enough sensitivity to probe a significant part of the parameter space of the CMSSM. In figure 6 an estimate of the flux sensitivity of the MAGIC Telescope currently under construction on the Canary Island La Palma [48] is shown in comparison to the flux predictions for the channel $\chi\chi \rightarrow \gamma\gamma$ for a large number of CMSSM models [47]. In addition figure 7 shows the expected coverage

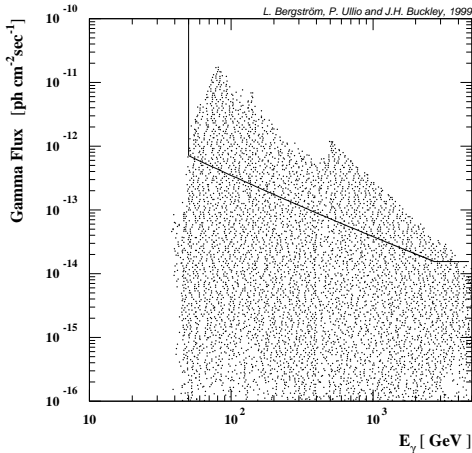


Figure 6. Flux sensitivity (5σ in 50 h observation time) of the upcoming MAGIC Telescope (full line) for a γ -ray source at the position of the GC compared to flux calculations within CMSSMs. Each point represents the prediction for one possible CMSSM model representation. All points satisfy $0.025 \leq \Omega_\chi h^2 \leq 1$. From [47].

for the CMSSM parameter space covering the DAMA evidence region illustrating the somewhat orthogonal sensitivity to the supersymmetric parameter space in terms of direct and annihilation cross section coverage for the same mass range.

A final remark on the DM problem: recent de-

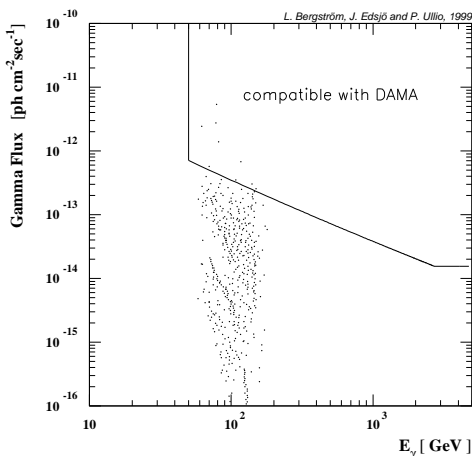


Figure 7. As for figure 6 but only the flux predictions for those CMSSM models are shown which predict a scalar elastic scattering cross section compatible with the DAMA evidence contour. From [49].

velopments in experimental and phenomenological Particle Physics point towards the fact that the existence of the observed baryon asymmetry itself is a signature of physics beyond the Standard Model. Csikor et al. showed in a 4-dim. lattice calculation [51, 52] that there is no first order electroweak phase transition in the Standard Model if $m_{\text{Higgs}} \gtrsim 75$ GeV. The critical point in the phase diagram of the electroweak phase transition is thus below the current lower Higgs mass limit from LEP II [53]. Therefore one of Sacharovs conditions for producing the observed baryon asymmetry (baryon number violation, CP violation, and out-of-equilibrium dynamics as in a first order phase transition) is not fulfilled for the electroweak symmetry breaking phase. Another mechanism which may be responsible for the baryon asymmetry and which has received growing attention lately due to the experimental evidence for a non-zero neutrino mass, is the leptogenesis mechanism [54]. In this model the cosmological baryon asymmetry is generated from a primordial lepton asymmetry which was produced by the out-of-equilibrium decay of heavy Majorana neutrinos. In a leptogenesis scenario Bolz, Plümacher and Buchmüller [55] showed that without encountering the 'gravitino problem' the non-baryonic DM might be present in the form of gravitinos (as the lightest supersymmetric particle) with masses in the range between 10 GeV and 100 GeV. This would mean that the nonbaryonic DM would be present as GIMPs, i.e., Gravitationally Interacting Massive Particles, in which case all laboratory searches would be negative and only astronomy, e.g., through weak gravitational lensing and ML, could provide more data on the DM.

3. Cosmic Rays and Antimatter

In the last years advancements in detector technology have led to an intensified study of many aspects of Cosmic Ray physics. With the upcoming Cosmic Ray (CR) experiments like, e.g., AUGER, AMS, and PAMELA, and the upcoming γ -ray detectors, e.g., CANGAROO II, GLAST, HESS, MAGIC, and VERITAS, it is safe to predict that this trend will continue (see also section 4). As the 'beam' of CRs is either background or signal the understanding of the CR spectrum and composition is of utmost importance for many current and upcoming astroparticle physics experiments.

Here we only report on some selected results and a few of the upcoming experiments focusing on the low energy and highest energy part of the measured CR energy spectrum. In the low energy domain the interest in CR measurements, beyond the

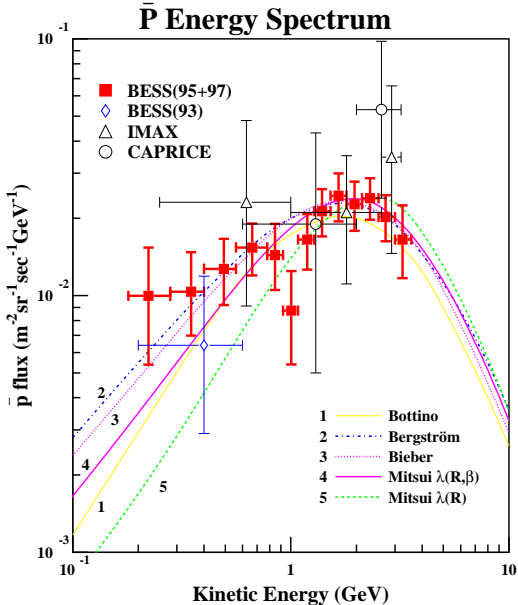


Figure 8. BESS 1995 and 1997 (solar minimum) antiproton fluxes measured at the top of the atmosphere. Also shown are some of the previously existing data. The error bars correspond to the quadratic sums of the statistical and systematic errors. The curves represent some recent calculations of the expected spectra from CR interactions with interstellar matter for the solar minimum period. From [56].

understanding of the sources and propagation of the CRs themselves, is focussed on the derivation of the neutrino oscillation parameters, the measurement of the antiproton and positron fluxes in the search for neutralinos and primordial black holes, and the search for antimatter.

A large fraction of past and present data on the absolute CR flux come from balloon-borne experiments. A representative detector flown in this type of experiment is the Japanese BESS spectrometer. The main parameters and components of this detector are the 1 Tesla magnetic field produced by a thin (4 g/cm²) superconducting coil filling a tracking volume equipped with drift chambers providing up to 28 hits per track with an acceptance of 0.3 m² sr. In addition two hodoscopes provide dE/dx and time-of-flight measurements. In the 1997 flight data at the top-of-the-atmosphere (mean residual air mass 5.3 g/cm²) were collected for 57,000 s. The combination of the measured \bar{p} fluxes as a function of kinetic energy from the 1995 and 1997 campaigns are shown in figure 8 [56].

Antiprotons should be produced as secondaries in interactions of the galactic CR protons with the interstellar medium. Their kinetic energy spectrum is expected to show a characteristic peak around 2 GeV, with sharp decreases in flux towards smaller and larger energies. Other possible sources of \bar{p} are the annihilation of neutralinos at the GC or the evaporation of primordial black holes (PBH). The latter possibility received growing attention in the recent past following the detection of antiprotons with kinetic energies below 0.5 GeV by BESS in 1993 [57]. Today black holes are only expected to be formed in stellar collapses of stars with several solar masses. The uniformity of space-time precludes collapses of matter to black holes with masses below this limit. In the early Universe, however, virulent conditions may have led to the formation of PBH with arbitrarily small masses [58], e.g., by the collapse of large density perturbations [59, 60]. Data constraining PBH abundances will thus yield constraints on the density fluctuation spectrum in the early Universe, an important ingredient of structure formation theories. Quantum effects lead to the evaporation of these PBH by particle emission [61]. The emission spectrum is similar to a black body with finite size and a temperature

$$T_{PBH} = \frac{\hbar c^3}{8\pi G M_{PBH}} = 1.06 \left(\frac{10^{13} \text{g}}{M_{PBH}} \right) \text{GeV}$$

where M_{PBH} is the mass of the PBH in grams. For T_{PBH} above the QCD-scale of ~ 300 MeV the evaporation process will result in relativistic quarks and gluons which may produce antiprotons during hadronisation. The expectation for the flux of antiprotons from this process is a spectrum increasing towards lower kinetic energies down to ~ 0.2 GeV [62]. Similarly the spectrum of \bar{p} expected from the annihilation of neutralinos at the GC is characterized by a significant flux below 1 GeV [63]. The uncertainty of the expected secondary flux due to the uncertainty of CR propagation in the Galaxy, however, is still of the same order of magnitude as the 'signal' expected from neutralino annihilation.

This propagation uncertainty is illustrated in figure 8. The data points show that BESS now has convincingly measured the predicted peak in the kinetic energy distribution at ~ 2 GeV. The location and height of this peak can be calculated by using the measured p and He CR spectra together with the cross sections for \bar{p} production measured at accelerators. The different propagation model calculations shown in figure 8 differ mainly in propagation parameters. Although the data below 2 GeV now are much better from the

statistical point-of-view, the uncertainty in the propagation of secondary \bar{p} s still precludes any firm conclusion on additional 'direct' sources of \bar{p} s. Future measurements at times with higher solar activity will be performed, e.g., by BESS, in order to study the secondary component in more detail. At times of high solar activity the 'direct' \bar{p} component should be virtually absent. In addition extending the measurements to larger energies (i.e., $E_{kin} \gg 2$ GeV) will also yield constraints on the propagation models. Here the current experiments did not have enough sensitivity and exposure to limit the propagation parameters. Upcoming CR experiments like, e.g., the PAMELA experiment, will here yield much improved data. PAMELA [64] is a satellite-borne magnet spectrometer currently being built by the WIZARD collaboration together with Russia. It is planned to be launched from Baikonur in 2002. The scientific objectives of the PAMELA mission are to measure the spectra of \bar{p} , e^+ , and nuclei in a wide range of energies, to search for primordial antimatter and to study the CR fluxes over half a solar cycle. PAMELA will be able to measure particles with magnetic rigidities (momentum/charge) up to a few hundred GV/c.

Contrary to the antiproton signal the positron signal from neutralino annihilation at the GC is expected to show up at large kinetic energies, i.e., well above the geomagnetic cutoff. The expectations for improved data in this channel from the upcoming experiments are also high. Similar to the antiproton channel the current data base on CR positrons does not yet allow any conclusion on additional sources besides CR interactions in the interstellar medium.

Another important aspect of CR physics is the search for primordial antimatter. This search mostly focuses on antihelium nuclei and currently the upper limit on the CR anti-helium/helium ratio provides the best evidence for the Galaxy and the nearby Universe being made up solely of matter. The combination of the BESS collaboration data taken during 5 campaigns between 1993 and 1998 have led to an improvement of the upper limit on the ratio of the abundances of antihelium to helium with magnetic rigidities between 1 GV/c and 16 GV/c by about a factor of 90 [65]. The upper limit of 10^{-6} quoted by BESS is compatible with the limit presented by AMS [4] and any further substantial improvement will need long duration measurements, e.g., by PAMELA or AMS.

The absolute fluxes of proton, helium and atmospheric muons are important for the derivation of the neutrino oscillation parameters since the atmospheric neutrino flux is proportional to the normalization of the dominating CR proton and

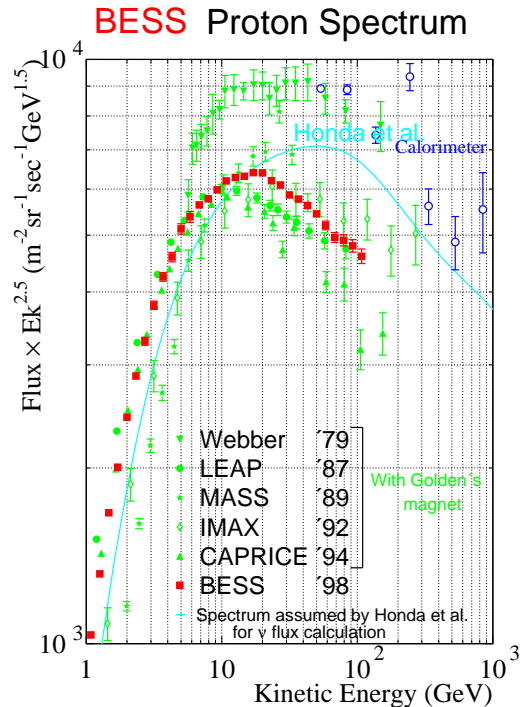


Figure 9. The absolute differential CR proton spectrum as measured by the BESS collaboration in 1998. Also shown are some previous measurements, and, as the full line, the spectrum assumed in the Honda *et al.* [66] calculation of the atmospheric neutrino fluxes. From [67].

helium fluxes. In addition there are other applications where the absolute measurement of the proton spectrum is important, e.g., in predictions of the secondary antiproton and positron fluxes needed to constrain exotic production channels and the above-mentioned propagation models.

Figure 9 shows the most recent measurement of the CR differential proton spectrum in the kinetic energy range between 1 GeV and ~ 100 GeV by BESS together with data taken by previous experiments [67]. Shown as the full line is the proton spectrum assumed in the Honda *et al.* Monte Carlo calculation [66] used in the analysis of the SuperKamiokande data on atmospheric neutrinos [68]. The different data sets show discrepancies in the measured absolute fluxes as large as a factor of 2 at ~ 50 GeV. The absolute differential proton flux was also measured with the MASS balloon detector in 1991 but published only recently [69]. In addition the differential helium flux at the top of the atmosphere and the differential muon fluxes in the atmosphere as a function of

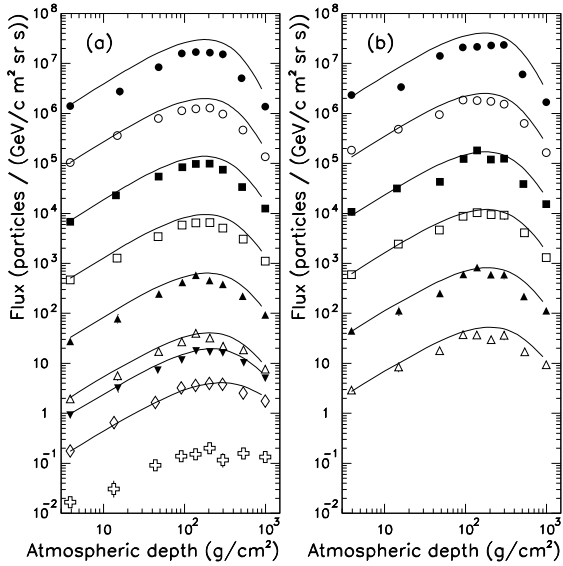


Figure 10. Differential (a) μ^- and (b) μ^+ fluxes as a function of atmospheric depth. From top to bottom the momentum ranges (in GeV/c) are: 0.3-0.53 (scaled by 10^5), 0.53-0.75 (10^4), 0.75-0.97 (10^3), 0.97-1.23 (10^2), 1.23-1.55 (10), 1.55-2 (1), 2-3.2 (1), 3.2-8 (1), and 8-40 (1). The μ^+ data are shown up to 2 GeV/c. The solid lines represent the Bartol Monte Carlo calculation results [73]. From [72].

atmospheric depth were measured. The proton and helium fluxes above 10 GeV were found to be compatible with the LEAP '87 data [70] as shown for the proton case in figure 9 corroborating a lower normalization of the absolute proton and helium fluxes as compared to previous compilations of data, e.g., [71].

The CAPRICE94 balloon experiment measured the atmospheric muon flux as a function of atmospheric depth [72] and compared the data to calculations using the Bartol Monte Carlo [73] (figure 10). The disagreement between data and Monte Carlo prediction increases with atmospheric depth from about 1.1 ± 0.1 (stat.) ± 0.1 (syst.) for the ratio of simulation result to the measured μ^- flux at the top of the atmosphere up to $1.8 \pm 0.1 \pm 0.1$ at the maximum of the muon flux at a depth of around 200 g/cm^2 . As the atmospheric muon flux is closely related to the flux of atmospheric neutrinos [74] these data will have to be used to improve the Monte Carlo generators. Gaisser investigated the influence of a change in slope and normalization of the input proton spectrum on the atmospheric neutrino result [75]. He concluded that for a change in the flux normalization above 10 GeV from the

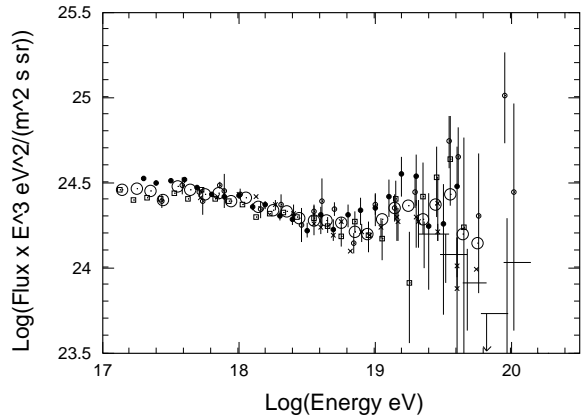


Figure 11. The top end of the CR energy spectrum as measured by AGASA, Fly's Eye, Haverah Park, and Yakutsk. The consistency of the spectrum is illustrated by the fact that only a shift in the absolute energy scale of $\sim 15\%$ was necessary in order to align the spectra. Note that the measured flux values were multiplied by E^3 to enhance the 'ankle' feature at around 10^{19} eV . From [76].

flux assumed by Honda *et al.* [66] in the direction of the new BESS result the observed excess of electron neutrinos would be increased by a similar amount and the deficit of muon neutrinos correspondingly reduced. Taking these new data into consideration in the fit of the SuperKamiokande data will very likely yield a shift in the fit parameters. Such a shift could be of great importance for the upcoming long-baseline neutrino experiments and illustrates the strengthening of the interconnection of Particle Physics and Astroparticle Physics in the search for New Physics.

At the uppermost end of the CR energy spectrum in the past 40 years a number of experiments have been collecting events with energies larger than 10^{18} eV . The galactic magnetic field ($B \sim 3 \mu\text{G}$) cannot contain CR protons with momenta larger than a few times $10^{18} \text{ eV}/c$. CRs with momenta above this value are thus very likely of extragalactic origin. Figure 11 shows a compilation of the all-particle flux above 10^{17} eV as measured by the four experiments AGASA, Fly's Eye, Haverah Park, and Yakutsk until 1995 [76]. The highest recorded CR energy to date is $3 \times 10^{20} \text{ eV}$ [77]. Of the four experiments which contributed to figure 11 the AGASA (Akeno) group has reported new results this year. The Akeno 20 km^2 air shower array was operated in Japan from 1984 to 1990 and became part of the still operational $\sim 100 \text{ km}^2$ Akeno Giant Air Shower Array (AGASA) in

1990. The detection of an anisotropy in the arrival direction of CRs with energies around 10^{18} eV ($0.8 - 2 \times 10^{18}$ eV) was reported by AGASA in 1998 [78] and updated recently [79]. The amplitude of the anisotropy in the first harmonic analysis was found to be 4% and could be identified in a 2-dimensional map as stemming from 4.5σ and 3.9σ excesses from the direction of the Galactic Centre and the Cygnus region, respectively. This is a spectacular result as it is clear evidence for the existence of galactic CRs up to this very high energy. Two possible explanations for the observed anisotropy were put forward. One is connected to the propagation of CR protons expected in direction of the nearby spiral arm. The other is that the anisotropy might be due to neutron primaries. At energies of 10^{18} eV neutrons have decay lengths of ~ 10 kpc and could thus propagate linearly from the GC and Cygnus regions to the position of the earth without decaying. More data are needed to distinguish between or rule out the models. At larger energies the AGASA collaboration did not detect any significant large-scale anisotropy with respect to the galactic or supergalactic plane [80]. The analysed event statistics was 581, 47, and 7 events with energies larger than 10^{19} eV, 4×10^{19} eV, and 10^{20} eV, respectively.

The size of the detectors and the time scale involved in collecting the data reported on above implies that only a new and bold ansatz will allow to improve the event statistics in a significant way. Especially at the uppermost end of the CR energy spectrum where 'New Physics' might be required to explain the data, at least an order of magnitude improvement in statistics is called for. Currently the world statistics of events with energies above 4×10^{19} eV is about 200 events corresponding to a total integrated exposure of ~ 1500 km².yr.sr. This energy is called the Greisen-Zatsepin-Kuzmin (GZK) cutoff energy and corresponds to the proton energy for which the centre-of-mass energy in a collision with a cosmic microwave background (CMB) photon crosses the pion photoproduction threshold, i.e.,

$$p + \gamma \rightarrow p + \pi^0 \quad \text{or} \quad p + \gamma \rightarrow n + \pi^+.$$

The survival probability of ultrahigh energy CR (UHECR) protons of energies 8×10^{18} eV, 10^{20} eV, and 3×10^{20} eV after having traversed a distance of 20 Mpc in the CMB are 0.70, 0.55, and 0.12, respectively. Sources of the UHECRs thus have to be within the GZK volume in our cosmic vicinity, i.e., closer than 30 to 50 Mpc. The possible sources discussed in the literature range from nearby proton accelerators, i.e., powerful Active Galactic Nuclei

(AGN) [81], Gamma-Ray Bursts (GRBs) [82, 83], the decay of superheavy relic particles [84], a new stable supersymmetric hadron with a mass of a few GeV, e.g., the S^0 as a *uds*-gluino bound state which would have a much longer pathlength in the CMB than ordinary hadrons [85], to extremely high energy neutrinos which would annihilate with relic neutrinos to produce hadronic jets [86]. For all these types of sources the EHECRs should point back (within $\sim 5^\circ$) to their source(s) *if* the extragalactic magnetic fields are weaker than $\sim 0.1 \mu\text{G}$. Should these fields be stronger the only sources from above for which the directional information is retained are the new stable supersymmetric hadron and the extremely high energy neutrinos interacting in the vicinity of the earth. As recent determinations of the magnetic field strength within the local (Virgo) supercluster indeed point towards a local field strength of $\sim 0.5 \mu\text{G}$ (e.g., [87]) 'conventional' local sources like AGN or GRBs might be 'hidden' due to large magnetic deflections already over distances of the order of Mpc [88].

The experimental investigation of UHECRs will be lifted to a new level with the upcoming Pierre Auger experiment [89]. In March of 1999 the ground breaking ceremony for the southern detector took place in the Pampa Amarilla in Argentina. The detector will consist of ~ 1600 water Cherenkov tanks spread over ~ 3000 km² with a 1.5 km grid spacing. This air shower detector will be overlooked by three fluorescence detectors situated within the array. The acceptance of the detector above 5×10^{19} eV will be $\sim 14,000$ km².yr.sr. Full operation of the detector is planned for the beginning of the year 2003.

4. Gamma Astronomy

Gamma astronomy is the most recent addition to the spectrum of 20th century astronomy. This concluded the opening of the *complete* electromagnetic spectrum to astronomical observations. Currently γ -ray astronomy is performed by space-borne and ground-based γ -ray detectors in non-overlapping energy domains. The space-borne detectors measure in the energy domain up to ~ 10 GeV whereas the ground-based detectors are limited to photon energies *above* ~ 200 GeV. The remaining gap in the electromagnetic spectrum will be closed by the upcoming detectors from both sides, i.e., by the ground-based and space-borne detectors enlarging their energy coverage. The number of γ -ray sources detected so far is about 270 in the energy domain below 10 GeV [90] and 13 sources (with a varying degree of certainty) with $E_\gamma \gtrsim 200$ GeV [92]. Note

that about 2/3 of the γ -ray sources detected below 10 GeV have not yet been identified with known astronomical objects. This class of 'EGRET Unidentified Sources' thus is one of the main targets for upcoming γ -ray experiments.

Here we only report on some recent results from ground-based γ -ray astronomy, i.e., results obtained with Imaging Air Cherenkov Telescopes (IACTs). The IACT technique is based on the exploitation of the inherent differences of γ and (CR) hadron air showers developing in the atmosphere. As a function of energy a growing number of secondary particles in the air showers have energies in excess of the threshold energy of $E_{thres} \sim 21$ MeV (at sea level) above which Cherenkov radiation is produced by the passage of charged particles through air. The emission of the Cherenkov light is concentrated into a small angular region in the forward direction and each shower typically illuminates an area of $\gtrsim 5 \cdot 10^4$ m² on the ground. Positioning the IACT anywhere in this area will result in a detection of the incident particle. The different images of hadrons and photons allow background suppression factors of ~ 600 with stand-alone telescopes. The suppression factor is larger by about an order of magnitude when one points several (3 to 5) telescopes at the same source in the stereoscopic observation mode pioneered by the HEGRA collaboration at the Canary Island La Palma [91]. Note that due to the indirect detection of the γ -rays interferometry, however, is not possible. The angular resolution of IACTs for individual events is about 0.1 to 0.2° and the energy resolution is between 10 and 40%. As for the background suppression, using several detectors in stereoscopic mode to measure the shower parameters, at current energies ($E \gtrsim 200$ GeV) leads to improvements in both parameters [91]. The large effective area gained by the indirect detection is one of the major advantages of the IACT technique as it allows to detect very low γ -ray fluxes. The major drawback of this technique, on the other hand, is the low duty cycle. Most IACTs are only operated during dark and moonless nights resulting in a duty cycle of about 10%.

Due to the restricted field-of-views of the instruments (a few degrees times a few degrees) the observations can only be performed in the pointing mode. In this mode the telescopes are oriented at possible γ -ray sources with guidance from other wavelengths together with model predictions for the very high energy (VHE) γ -ray channel. One such model prediction concerns the important question of the origin of the CRs. In most models Supernova Remnants (SNRs) are the favoured sites of CR acceleration. As the CR nuclei themselves do

not retain directional information in the galactic magnetic field a neutral particle signal must be searched for in order to identify the CR sources. Whenever hadrons are accelerated to very high energies pions should be produced as secondaries. However, SNRs are known sources VHE γ -rays and the main γ -ray component is due to inverse Compton scattering of ultrarelativistic electrons on low energy photons (e.g., CMB photons). In order to identify the sources of the CRs one thus aims at identifying an *additional VHE γ -ray component* stemming from π^0 decay. SNRs thus have been intensively studied by the IACTs in the past. Although six SNRs have been observed above ~ 200 GeV [92] (Crab nebula, Vela, PSR1706-44, SN1006, REX1713.7-3946, and (possibly) CasA), this additional component has not been clearly identified, yet. More sensitive measurements at lower energies will be of great importance in identifying the spectral component(s) observed in the six sources above and to discover γ -ray emission in more SNRs. With low energy thresholds, e.g., of the upcoming MAGIC Telescope (initially 25 GeV), it may be possible to observe a *two component γ -ray spectrum*, which should then allow to decouple the predicted leptonic and hadronic components in SNR shells. In summary, no clear evidence for proton acceleration in SNRs was found up to now and the sources of the galactic CRs are not identified yet.

The most spectacular discoveries in ground-based γ -ray astronomy are related to the *extragalactic* sources of VHE γ -rays. The first such source discovered in 1992 by the Whipple collaboration [93] was the closest BL Lacertae (BL Lac) type object Markarian 421 (Mrk 421) at a redshift $z = 0.031$. This AGN at the same time is one of the weakest γ -ray source detected by the EGRET experiment at energies below ~ 10 GeV [90] and showed the shortest time variations of its γ -ray emission levels observed so far with doubling and decaying times in the energy domain above ~ 200 GeV as short as 15 minutes [94]. The amplitude ratios between the discovery flux level and flux maxima during short outbursts have been as large as 30, i.e., between 0.3 and 10 Crab, where 1 Crab is the (time-independent) flux of the standard candle of γ astronomy, the Crab nebula.

BL Lac objects and flat spectrum radio-loud quasars (FSRQs) are collectively called "blazars". The predominantly non-thermal emission shows violent variability in most energy bands and superluminal motion is observed in VLBI radio surveys. The non-thermal emission is believed to originate in relativistic jets oriented with small angles towards the line of sight. The emission levels and time scales observed in the TeV domain, e.g.,

for Mrk 421, clearly show that *relativistic beaming* has to be operational in the sources, corroborating this model picture. The ultimate energy source is believed to be gravitational, i.e., originating from accretion of matter onto a supermassive ($\mathcal{O}(10^8 - 10^9) M_{\odot}$) black hole in the centre of the AGN. How the jets are formed or how they are fueled is not yet understood. One viable model is based, e.g., on the extraction of the rotational energy from the ergosphere of the (\sim maximally) spinning black hole [95]. Irrespective of the actual formation and fueling of the jet there are two models put forward to explain the observed radiation from γ -ray emitting blazars.

The spectral energy distributions of blazars in general seem to consist of two parts. First, a low energy component rising from the radio up to a broad peak between the infrared (IR) and X-ray wavelengths (see, e.g., figure 13) depending on the specific blazar type. This component is generally believed to stem from incoherent synchrotron emission by relativistic electrons in the jets. The origin and composition of the high energy component, however, is still a matter of debate. Most popular is the model in which the γ -rays are produced in optically thin regions through inverse Compton scattering of low energy photons by the same electron population that produces the synchrotron emission. Different models of this type differ, e.g., in the origin of the low energy seed photons. These photons can be synchrotron photons (Synchrotron Self Compton Model), photons from the accretion disk, or other photons in the vicinity of the jet (External Compton Models) (e.g., [96]). In a different type of model VHE γ -rays are produced by proton-initiated cascades (PIC) [97]. In this case normal plasma is injected into the jet and shocks within the jet accelerate protons and electrons to very high energies at which pions can then be photoproduced. All or parts of the VHE γ -ray emission in this case is the end product of an electromagnetic cascade developing in an optically thick acceleration region. Note that this model was the only one *predicting* γ -ray emission to energies up to and beyond 20 TeV. A common denominator of all models is that the γ -rays originates close to the central black hole. Should the low energy fields near to the accretion disk, however, be very intense the direct escape of the γ -rays becomes difficult due to $\gamma\gamma \rightarrow e^+e^-$ pair production losses [98]. VHE γ -ray data on time variability and energy spectra taken concurrently with data in other energy bands will help to constrain or rule out the models.

The second extragalactic source, Mrk 501, was discovered in 1995 [99] as a weak source (0.08 Crab).

In the beginning of 1997 it showed a dramatic outburst at TeV energies which lasted for the full 1997 observation period (March - September) and was characterized by wildly varying emission levels. The most complete light curve at energies larger than 1.5 TeV was obtained by the 6 IACTs of the HEGRA collaboration who operated at that time a stereoscopic system of 4 IACTs and 2 additional stand-alone telescopes. In order to achieve this good time coverage of Mrk 501 for the first time measurements during moon time were performed with one of the stand-alone telescopes (CT1) [100]. This observation mode considerably increased the time coverage with only a moderate increase in energy threshold. The light curve measured by all HEGRA IACTs is depicted in figure 12 (top diagram). Concurrently with HEGRA and many other IACTs (e.g., [101]) the Allsky Monitor (ASM) of the RXTE X-ray satellite took data on Mrk 501 in the 2 to 10 keV energy band. The corresponding light curve is also shown in figure 12 (bottom diagram). HEGRA performed a correlation analysis and found a moderate (0.611 ± 0.057) but clear (8.5σ) correlation between the TeV and keV emission levels [102] indicating a common emission region of the radiation.

The determination of the velocity of this emitting region within the jet also illustrates the impact of such concurrent observations. The bulk Lorentz factors, γ_{bulk} , of the relativistically moving plasma can be determined in two independent ways. From radio observations with the Space-VLBI technique for Mrk 501 the inclination of the jet axis with the line of sight was measured to be $\Theta \sim 10^\circ - 15^\circ$. At the same time the bulk velocity of the synchrotron emitting plasma, β , was measured to be in the range from 0.990 to 0.999. These numbers can be translated into a Lorentz factor, γ_{bulk} , between 7 and 22 or a Doppler factor $\delta = [\gamma_{bulk}(1 - \beta \cos \Theta)]^{-1}$ between 1.3 - 5.6 [103]. The other method is based on the simultaneous observation of synchrotron spectra in the optical/UV domain and TeV γ -ray spectra and makes use of the Synchrotron Self Compton model. In this case the concurrent observations require $\delta \gtrsim 5$ [104] consistent with the radio determinations.

HEGRA investigated the X-ray and TeV light curves shown in figure 12 for quasi-periodic oscillations (QPOs) [105]. In the QPO analysis evidence for a 23 day period was found in both light curves. In order to assign a statistical significance a shot noise model assuming as null hypothesis independent, randomly distributed flares in accordance with observations was developed [106]. The combined probability

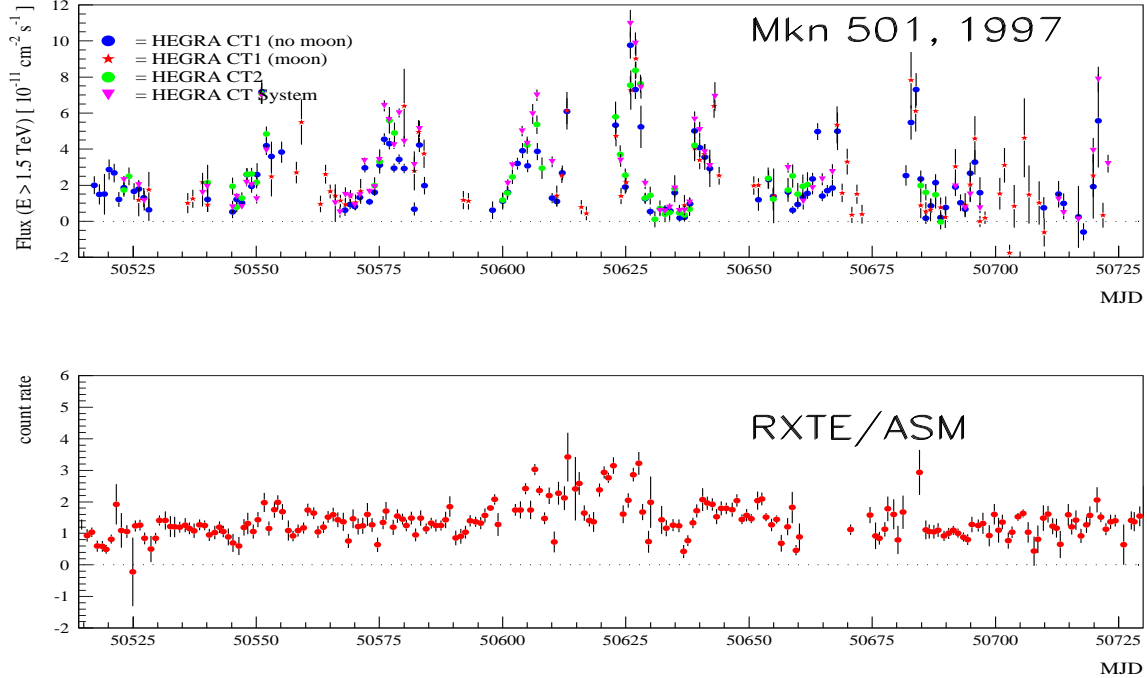


Figure 12. Light curves of Mrk 501 in 1997. Top: VHE γ -ray (> 1.5 TeV) emission measured by the HEGRA IACTs. Modified Julian Day 50449 corresponds to January 1, 1997. Bottom: X-ray light curve measured by the RXTE ASM for $2 \text{ keV} \leq E \leq 10 \text{ keV}$. From [102].

for the 23 day period was thus determined to be $\mathcal{P} = 2.8 e-04$ or 3.5σ . Note that this analysis was only possible because the data taken during moon time were available. Leaving out these data introduces large time gaps and the observed QPO signal will be washed out due to the introduction of aliasing effects. The interpretation of the observed 23 day period is complicated by the uncertainty of the exact location and environment of the emission region. It could be due gravitomagnetic precession or g-mode oscillations of the accretion disk in analogy to models put forward to explain QPOs observed during X-ray flares of the galactic analog to AGN, the X-ray binaries [107]. Or it could be due to the action of a close binary system of supermassive black holes in the centre of AGN which is plausible based on the heavy galaxy merger activity, e.g., observed in the Hubble Deep Fields [108]. Other possibilities are radiating clumps on helical trajectories or oblique shock fronts.

Besides the light curve the other important measurement concerns the γ -ray energy spectra of AGN during high and low states. From their observations of Mrk 501 in 1997 the CAT collaboration determined energy spectra for different γ -ray intensities [109]. Figure 13 shows

an example of the multi-wavelength spectra of Mrk 501 as measured by the BeppoSAX X-ray satellite and the CAT telescope on April 7th and April 16th. The flux in the γ -ray band differs by about a factor of 10. In addition CAT found that the increase in flux was also accompanied by an increase in the spectral hardness [112]. At somewhat higher energies this trend could not be found in the HEGRA data [113]. The most striking aspect of the HEGRA energy spectrum of Mrk 501 in 1997, besides its independence from the flux level, is the maximum energy observed from this source. This energy spectrum together with the energy spectrum determined for Mrk 421 from the combined 1997 and 1998 data is shown in figure 14. The 95% CL lower limit on the maximum detected energy from this extragalactic source is 16 TeV! Due to the distance of Mrk 501 of about 500 million light years the measurement of this maximum energy is a cosmologically important signal. The reason for this is that the TeV γ -rays have to traverse the diffuse extragalactic background light (EBL) in order to arrive at the location of our Galaxy. The EBL constitutes an important cosmological signal as it integrates over the emission history of the Universe on Hubble

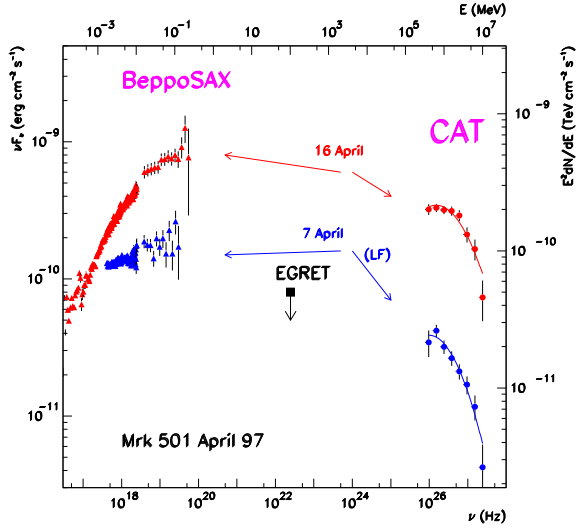


Figure 13. Mrk 501 X-ray and VHE spectra given as νF_ν . For April 7th and 16th, BeppoSAX data were taken from [110]. The EGRET upper limit was taken from [111] and corresponds to observations between April 9th and 15th. From [112].

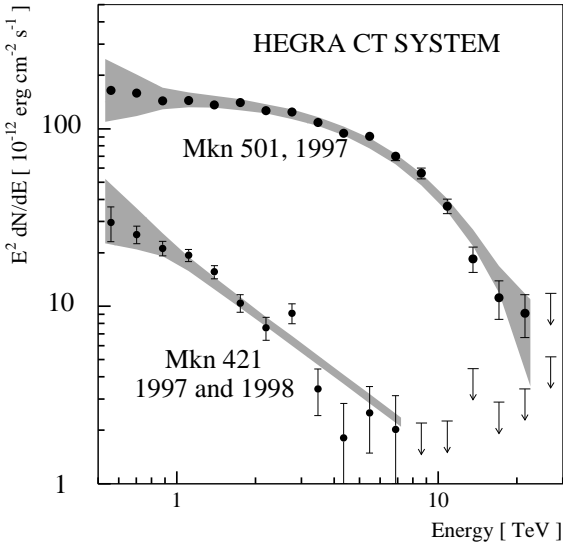


Figure 14. The energy spectra of Mrk 421 (1997 and 1998 combined) and Mrk 501 (1997) as measured by the system of HEGRA IACTs. From [113].

time and length scales. Important parts of the EBL spectrum, amongst others the infrared region, however, are still only known very poorly from direct measurements by satellite detectors. TeV γ -rays can interact with infrared photons to produce electron-positron pairs. A large density of diffuse infrared photons therefore results in measurable absorption features in extragalactic γ -ray spectra. As the energy dependence of the EBL flux is roughly $\propto E^{-1}$ quasi-exponential cutoffs of the TeV spectra are expected. By turning this argument around one sees that a beam of TeV γ -rays traveling cosmological distances can be used to probe this background field. As the relevant Thomson cross section is strongly peaked at the threshold this probing can even be performed spectroscopically by observing sources at different distances. Because of the energy dependence of the EBL spectrum the cutoff condition, i.e., optical depth reaching unity, for sources at different cosmological distances occurs at different γ -ray energies. A 'cosmological γ -ray horizon with the Universe opening up as one goes towards lower γ -ray energies should result. A small fraction of the EBL spectrum is shown in figure 15. What is striking is that in the shown energy interval between the far infrared ($\sim 200 \mu\text{m}$) and the ultraviolet (UV) ($\sim 0.1 \mu\text{m}$) the figure is dominated by wildly scattered upper and lower limits. The main reason for this is the enormous foreground radiation in this spectral range by the zodiacal light in our solar system. Besides the limits and measurements obtained with 'direct' methods also the upper limits on the IR EBL level derived from the TeV γ -ray spectrum of Mrk 501 as measured by the Whipple collaboration is shown in figure 15. A similar analysis was performed on the basis of the HEGRA data resulting in an upper limit of $1.1 \times 10^{-3} \text{ eV/cm}^3$ at $\sim 25 \mu\text{m}$ assuming a specific shape of the IR background [23]. As visible in figure 15 the application of the methods of TeV γ -ray astronomy have already led to an improvement of the upper limits in the mid-infrared range by more than an order of magnitude.

Especially in the mid-infrared range where the models predict a pronounced dip in the diffuse extragalactic photon flux the dominating foreground will also in the future probably not allow a certain direct determination of the flux level by infrared satellites. The level of the EBL in this range, however, is an important signal of structure formation in the Universe and constitutes a (complicated) convolution of star formation rate, initial mass function and its evolution, and the dust history of the Universe. It is therefore of paramount interest to determine the flux with the methods of TeV astronomy. As this means measuring cutoff

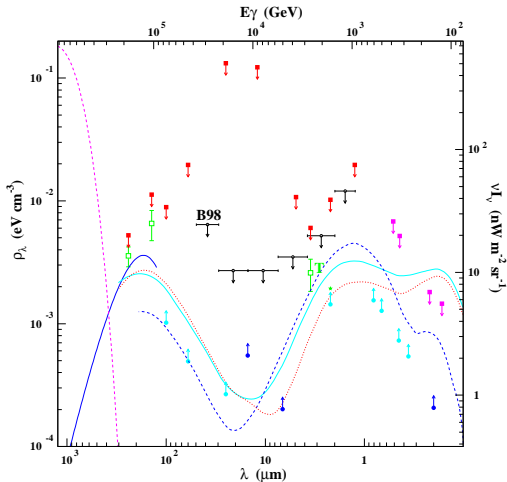


Figure 15. The density of the EBL between the far-infrared and the ultraviolet. Filled squares with arrows indicate 95%CL upper limits by various experiments. Open squares are detections (140 and 240 μm) and a tentative detection (3.6 μm , denoted by T) by DIRBE. The filled circles are lower limits from IRAS and ISO galaxy counts. For references see [114]. The horizontal bars with arrows indicate the upper limits from the Mrk 501 spectrum derived in [115]. The dashed line above 300 μm indicates the level of the 2.7K CMB. The dotted and dot-dashed lines are model predictions from [116] and the dashed line a prediction taken from [117]. From [114].

energies in the TeV domain, it makes it necessary to find more close-by (on cosmological scales) TeV sources, i.e., raising the instruments sensitivities as planned for the next generation of γ -ray detectors.

The final result from TeV γ -ray astronomy reported on here concerns the test of Lorentz invariance made possible by the combination of high energy emission and cosmological distances. Some of the ansätze for Quantum Gravity (QG), e.g., [118], yield non-Lorentz-invariant terms which lead to modified laws of propagation and interaction of neutral particles as a result of interactions with the quantum gravity medium. Measurable time delays can be expected if the particles have energies close to the QG scale (expected to be close to the Planck scale, i.e., 10^{19} GeV) or if they have traversed cosmological distances. Biller et al. [119] analysed the shortest flare of Mrk 421 observed on May 15 1996 by the Whipple collaboration [94] for a time delay between γ -rays with energies less than 1 TeV and those with energies above 2 TeV. No difference was found within the measurable shortest time bin of 280 s and a lower limit of 4×10^{16} GeV could be placed on the relevant QG energy

scale. In general this type of investigation can be used to place limits on any non-Lorentz invariant propagation term. By searching for effects of this kind in very intense transient phenomena occurring at cosmological distances like, e.g., GRBs, the upcoming MAGIC telescope will have sensitivity at the Planck scale [120]. For comparison, the current best limits are about 1% of the Planck scale.

5. Neutrino Astronomy

The observation of low energy astrophysical neutrinos from the sun and SN1987A has led to important astrophysical and particle physics results. The fundamentally new aspect of performing neutrino astronomy in contrast to astronomy with electromagnetic radiation lies in the penetration power of neutrinos, i.e., also optically thick regions can be studied in the neutrino 'light'. In addition neutrinos do not suffer attenuation losses due to absorption on background radiations as do γ -rays or ultrahigh energy hadrons. We know from the observation of CRs that large numbers of hadrons are accelerated to very high energies in astrophysical environments. Whenever processes accelerate hadrons to VHE energies besides the production of γ -rays we naturally expect neutrino fluxes as least as large as the γ -ray fluxes and neutrino and γ -ray astronomy are complementary approaches to many astroparticle physics questions. Also several astrophysical events, e.g., supernovae (SN) or GRBs, are predicted to emit their maximum power in the neutrino channel. In summary, all environments where photoproduction of pions is likely to occur are potential high energy neutrino sources. These are the (unknown) sources of CRs, the jets of AGN if protons are accelerated within the jets, the Galactic disk because of CR interactions with the interstellar matter, or the centres of galaxy clusters where UHECRs might be present. In addition there are exotic sources like the pairwise annihilation of neutralinos and radiation from topological defects. Note that the detection of AGN as point sources for high energy neutrinos is considered to be the *experimentum crucis* in distinguishing between jet models where only electrons and positrons or where 'normal plasma', i.e., electrons and protons produce the observed VHE γ radiation. Although the neutrino-proton cross section rises linearly up to energies of $\sim 10^8$ GeV before flattening due to W propagator effects the strongly falling fluxes expected from most conceivable sources demands that high energy neutrino detectors have to be huge instruments. For more information and the potential of this exciting new field see, e.g., [122, 123].

The instruments that are taking data (BAIKAL, AMANDA-B13), are under construction (AMANDA-B, ANTARES Phase II), or are in the test phase (NESTOR) are huge detectors with effective collection areas between 2×10^3 and $\sim 10^5$ m². Due to the expected low rates, however, all these detectors are considered to be first or second steps towards the construction of one or two 1 km³ detectors (e.g., ANTARES, ICECUBE, NESTOR). Basically the detectors are muon detectors aimed at measuring ν_μ and $\bar{\nu}_\mu$ induced *upward going* high energy muons. At high energies this gives the added advantage of enlarging the fiducial volume of the detectors due to the long range of high energy muons in water or ice. Water or ice are the detector media of choice because the detection of the muons utilizes the Cherenkov light emitted by the water or ice when traversed by relativistic particles with energies above the Cherenkov threshold. The main parameters of these neutrino telescopes are the angular and energy resolution. In general water detectors will have a better angular resolution but worse energy resolution compared to ice detectors. In addition ν_e and $\bar{\nu}_e$ fluxes can be easily measured at large energies based on the detection of induced electromagnetic showers. The major background to extraterrestrial neutrinos is given by the *downward going* atmospheric neutrinos and the *upward going* muon flux induced by atmospheric neutrinos both of which are produced by the interaction of CRs in the earth's atmosphere. In addition to constituting two sources of background, however, these two beams can be used as test beams for proving the feasibility of these detectors by measuring the fluxes and angular distributions of these beams at very high energies.

An ice detector currently under construction is the AMANDA-B detector at the South Pole. It will have an effective collection area of 10,000 m², an energy threshold of ~ 50 GeV and an angular resolution of about 2.5° per muon track [123]. While being constructed at different depths the AMANDA detector has been taking data. The AMANDA-A detector was installed in a depth between 810 and 1000 m below the south pole's surface and is characterized by a high concentration of residual air bubbles leading to strong scattering of light. While this dramatically worsened the angular resolution it improved the calorimetric performance and the 1995 data cascade trigger data of AMANDA-A could be used to put an upper limit on the diffuse flux of $\nu_e + \bar{\nu}_e$ in the energy range from 10^4 to 10^7 GeV [124]. Due to the small size of AMANDA-A this limit is, however, not yet restricting the model space of fluxes predicted in AGN models (see figure 16). After AMANDA-A the installation

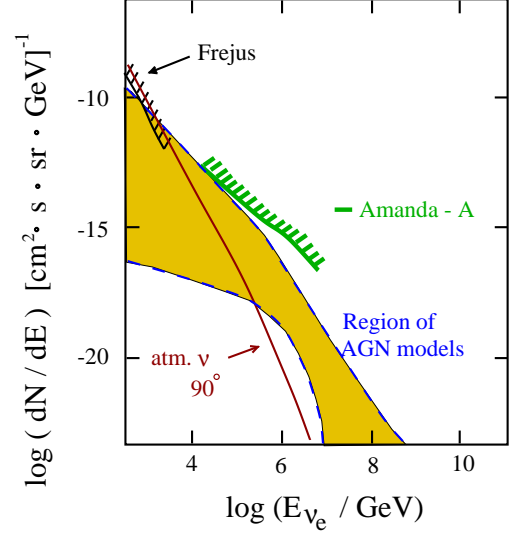


Figure 16. Limits on the diffuse $\nu_e + \bar{\nu}_e$ flux as determined by the Frejus [125] and AMANDA-A detectors. From [124].

towards the AMANDA-B detector started with the deployment of 4 strings at a depth between 1.5 and 2 km. For results from this detector see [126]. The data taken during the first year of operation of the 10 string AMANDA-B10 detector installed in the depth between 1500 and 1980 m were analyzed for upward going muon candidates [127]. In a preliminary analysis of data taken during 113 days 17 events passed all selection cuts. This corresponds to a reduction of the number of events in the solid angle where the 'pencil like' AMANDA-B10 detector is sensitive by more than a factor of 10^5 . The result was found to be in accordance with the Monte Carlo expectation of 21.1 events. The reconstructed zenith angle distributions for the full data set (4.9×10^8 events), and the data sets after different selection cuts are shown in figure 17.

The BAIKAL detector, operational since April 1993, also took data while being enlarged to its final NT-200 configuration in April 1998. BAIKAL can be considered to be the water detector which proved the feasibility of very high energy neutrino telescopes when it reconstructed the first two atmospheric neutrino candidates from the initial NT-36 data taken between April 1994 and March 1995 [128]. In its NT-96 configuration it took data from April 1996 until March 1997 and a very tight limit could be placed on the diffuse $\nu_e + \nu_\mu$ flux for neutrino energies larger than 10 TeV [129]. This limit together with some other experimental

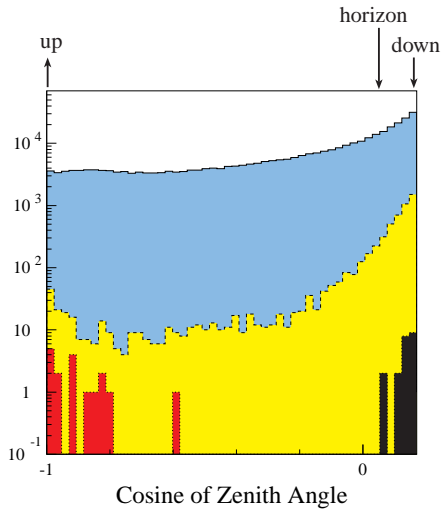


Figure 17. Reconstructed zenith angle distributions of 113 days of AMANDA-B10 data after quality cuts tightening from top to bottom. The 17 events with a $\cos\theta_{zenith}$ close to -1 are atmospheric neutrino candidates. From [127].

limits and model predictions is shown in figure 18. Although the BAIKAL NT-96 limit is still about a factor of 10 above the highest model predictions it demonstrates the capability of the underwater technique. This technique is also going to be applied by the ANTARES project planning the construction of a 1 km³ detector in the Mediterranean Sea (e.g., [131]). Since 1997 ANTARES is conducting an intense R & D program aimed at the installation of a 0.1 km² detector in ANTARES Phase II by 2002 to 2003. In this approved phase 13 strings with ~ 1000 PMTs will be deployed in about 2500 m depth. Monte Carlo simulations of the performance look very promising, e.g., an angular resolution of $\sim 0.2^\circ$ is indicated.

6. Outlook

The major potential of Astroparticle Physics is given by the synergistic effects of combining particle, nuclear and atomic physics with astrophysics and cosmology and it has started to make an impact on important physics questions. The improvement of detector technology coupled with improved 'calibrations' of astrophysical beams, e.g., CR fluxes or γ and ν fluxes from extragalactic objects, will lead to an even larger sensitivity to fundamental questions in the future.

References

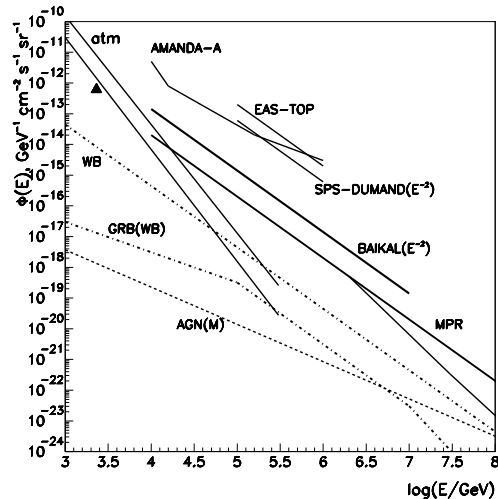


Figure 18. Upper limits on the differential flux of high energy neutrinos obtained by different experiments and some upper bounds on neutrino fluxes for different models. For full references see [129]. Dot-dash curves labeled WB and GRB(WB) - upper bound and neutrino intensity from GRB estimated by Waxman and Bahcall [121]; dashed curve labeled AGN(M) - neutrino intensity from AGN (Mannheim, model A [130]); solid curves labeled MPR - upper bounds for $\nu_\mu + \bar{\nu}_\mu$ in [130] for pion photo-production neutrino sources with different optical depth τ . The triangle denotes the limit obtained by Frejus for an energy of 2.6 TeV : $7 \cdot 10^{-13} \text{cm}^{-2} \text{s}^{-1} \text{sr}^{-1} \text{GeV}^{-1}$ [125]. From [129].

- [1] Maggiore M 1999, *Phys. Rep. to appear*, Electronic preprint gr-qc/9909001
- [2] Jung C K 1999 These proceedings
- [3] *Proc. of 26th ICRC, Salt Lake City*
- [4] Hofer H 1999 These proceedings
- [5] Turner M S and Tyson J A 1999 *Rev. Mod. Phys.* **71** S145
- [6] Ries A et al. 1998 *Astrophys. J.* **116** 1009
- [7] Perlmutter S et al. 1999 *Astrophys. J.* **517** 565
- [8] Rubin V C and Ford W K 1970 *Astrophys. J.* **159** 379
- [9] Olive K, Steigman G, Walker T P 1999 *Special memorial volume of Physics Reports in honor of David Schramm*
- [10] Paczyński B 1986 *Astrophys. J.* **304** 1
- [11] Roulet E and Mollerach S 1997 *Phys. Rep.* **279** 67
- [12] Aubourg E et al. 1993 *Nature* **365** 623
- [13] Alcock C et al. 1993 *Nature* **365** 621; *Astrophys. J.* **445** (1995) 133
- [14] Moniez M 1999 These proceedings

- [15] Afonso C et al. 1999 *subm. to Astrophys. J.* Electronic preprint astro-ph/9907247
- [16] Afonso C et al. 1999 *Astron. Astrophys.* **344** L63
- [17] Renault C et al. 1997 *Astron. Astrophys.* **324** L69
- [18] Alcock C et al. 1997 *Astrophys. J.* **486** 679
- [19] Gilmore G and Unavane M 1998 *Mon. Not. R. Astron. Soc.* **301** 813
- [20] Freese K, Fields B and Graff D S 1999 *Proc. 19th Texas Symposium on Relativistic Astrophysics and Cosmology, Paris*, Electronic preprint astro-ph/9904401
- [21] Fields B, Freese K, Graff D S 1998 *New Astron.* **3** 347
- [22] Fields B, Freese K, Graff D S 1999 *subm. to Astrophys. J.*, Electronic preprint astro-ph/9904291
- [23] Funk B, Magnussen N et al. 1998 *Astropart. Phys.* **9** 97
- [24] Graff D S, Freese K, Walker T P, Pinsonneault M H 1999 *Astrophys. J.* **523** L77
- [25] De Paolis F, Ingrosso G, Jetzer Ph, Roncadelli M 1996 *Int. J. Mod. Phys.* **D5** 151
- [26] De Paolis F, Ingrosso G, Jetzer Ph, Roncadelli M 1999 *Astrophys. J.* **510** L103
- [27] Volkas R R 1999 *Proc. 8th International Symposium on Neutrino Telescopes, Venice*, Electronic preprint hep-ph/9904437
- [28] Peccei R and Quinn H 1977 *Phys. Rev.* **D16** 1791
- [29] Hagemann C et al. 1998 *Phys. Rev. Lett.* **80** 2043
- [30] Sikivie P 1999 *Proc. Axion Workshop, Univ. of Florida, Gainesville, Florida*, to be published in *Nucl. Phys. B (Proc. Suppl)*
- [31] Weinheimer Ch 1999 These proceedings
- [32] Klapdor-Kleingrothaus H V 1999 *Proc. Int. Conf. on Lepton- and Baryon Number Non-Conservation, Trento, Italy*, IOP, Bristol
- [33] Jungman G, Kamionkowski M, Griest K 1996 *Phys. Rep.* **267** 195
- [34] *Proc. VIIth Int. Workshop on Low temperature Detectors, Munich, 1997*, Max-Planck Institute of Physics, Munich
- [35] Bernabei R et al. 1998 *Phys. Lett.* **B424** 195
- [36] Bernabei R et al. 1999 *Phys. Lett.* **B450** 448
- [37] Bernabei R 1999 *CERN Courier* **39** 17
- [38] Baudis L. et al. 1998 *Phys. Rev.*, **D59** 022001
- [39] Akerib D S et al. 1998 *Nucl. Phys. B (Proc. Suppl)* **70** 64
- [40] Smith P F et al. 1998 *Phys. Rep.* **307** 275
- [41] Gerbier G et al. 1999 *Astropart. Phys.* **11** 287
- [42] Smith N J T 1999 These proceedings
- [43] Klapdor-Kleingrothaus H V 1998 *Int. J. Mod. Phys.* **A13** 3953
- [44] Bergström L and Snellman H 1988 *Phys. Rev.* **D37** 3737
- [45] Ullio P 1999 *Dissertation, Stockholm University, Department of Physics*
- [46] Urban M et al. 1992 *Phys. Lett.* **B293** 122
- [47] Bergström L, Ullio P, Buckley J 1998 *Astropart. Phys.* **9**
- [48] Lorenz E 1999 *Proc. GeV-TeV Workshop, Snowbird*
- [49] Ullio P 1999 Private communication
- [50] Ajima Y et al. 1999 *subm. to Nucl. Instrum. Methods.*
- [51] Csikor F 1999 These proceedings
- [52] Csikor F, Fodor Z, Heitger J 1999 *Phys. Rev. Lett.* **82** 21
- [53] Gross E 1999 These proceedings
- [54] Fukugita M and Yanagida T 1986 *Phys. Lett.* **B174** 45
- [55] Bolz M, Buchmüller W, Plümacher M 1998 *Phys. Lett.* **B443** 209
- [56] Yoshimura K et al. 1999 *Proc. of 26th ICRC, Salt Lake City* **3** 81
- [57] Yoshimura K et al. 1995 *Phys. Rev. Lett.* **75** 3792
- [58] Novikov I D et al. 1997 *Astron. Astrophys.* **80** 104
- [59] Zel'dovich Ya B and Novikov I D 1966 *Astron. Zh.* **43** 758
- [60] Hawking S W 1971 *Mon. Not. R. Astron. Soc.* **152** 75
- [61] Hawking S W 1974 *Nature* **248** 30
- [62] MacGibbon J H and Carr B J 1991 *Astrophys. J.* **371** 447
- [63] Bergström L, Edsjö J, Ullio P 1999 *Proc. of 26th ICRC, Salt Lake City*, **2** 285
- [64] Adriani O et al. 1995 *Proc. of 24th ICRC, Rome* **3** 591
- [65] Nozaki M et al. 1999 *Proc. of 26th ICRC, Salt Lake City* **3** 85
- [66] Honda M, Kajita T, Kasahara K, Midorikawa S 1995 *Phys. Rev.* **D52** 4985
- [67] Sanuki T et al. 1999 *Proc. of 26th ICRC, Salt Lake City* **3** 93
- [68] Fukuda Y et al. 1998 *Phys. Rev. Lett.* **81** 1562
- [69] Bellotti R et al. 1999 *to appear in Phys. Rev. D*, Electronic preprint hep-ex/9905012
- [70] Seo E S et al. 1991 *Astrophys. J.* **378** 763
- [71] Papini P, Grimani C, Stephens S A 1996 *Nuovo Cimento* **19C** 367

- [72] Boezio M et al. 1999 *Phys. Rev. Lett.* **82** 4757
- [73] Gaisser T K and Stanev T 1995 *Proc. of 24th ICRC, Rome* **1** 694
- [74] Perkins D H 1994 *Astropart. Phys.* **2** 249
- [75] Gaisser T K 1999 *Proc. Neutrino 98, Takayama, Japan, Nucl. Phys. Proc. Suppl.* **77** 133
- [76] Yoshida S et al. 1995 *Astropart. Phys.* **3** 105
- [77] Bird D J et al. 1995 *Astrophys. J.* **441** 144
- [78] Hayashida N et al. 1998 *Astropart. Phys.* **10** 304
- [79] Hayashida N et al. 1999 *Proc. of 26th ICRC, Salt Lake City* **3** 256
- [80] Takeda M et al. 1998 Electronic preprint astro-ph/9902239
- [81] Biermann P L and Strittmatter P 1987 *Astrophys. J.* **322** 643
- [82] Waxman E 1995 *Phys. Rev. Lett.* **75** 386
- [83] Vietri M 1995 *Astrophys. J.* **453** 883
- [84] Hill C et al. 1986 *Phys. Rev.* **D34** 1622
- [85] Chung D J H, Farrar G R, Kolb E W 1997 *Phys. Rev.* **D57** 4606
- [86] Weiler T 1997 Electronic preprint hep-ph/9710431
- [87] Kronberg P 1994 *Phys. Rep.* **57** 325
- [88] Farrar G R and Biermann P L 1999 Electronic preprint astro-ph/9906431
- [89] Boratov M, Cronin J W, Watson A A 1992 *Nucl. Phys. B (Proc. Suppl.)* **28B**
- [90] Macomb D J and Gehrels N 1999 *Astrophys. J. Suppl.* **120** 335
- [91] Daum A, Hermann G, Hess M et al. *Astropart. Phys.* **8** 1
- [92] Weekes T C 1999 *Proc. GeV-TeV Workshop, Snowbird* Electronic preprint astro-ph/9910394
- [93] Punch M et al. 1992 *Nature* **358** 477
- [94] Gaidos J A et al. 1996 *Nature* **383** 319
- [95] Blandford R and Znajek 1977 *Mon. Not. R. Astron. Soc.* **179** 433
- [96] Hoffman C M et al. 1999 *Rev. of Mod. Phys.* **4** 897
- [97] Mannheim K 1993 *Astron. Astrophys.* **269** 67
- [98] Protheroe R J and Biermann P L 1997 *Astropart. Phys.* **6** 293
- [99] Quinn J et al 1996 *Astrophys. J. Lett.* **456** L83
- [100] Kranich D et al. 1998 *Astropart. Phys.* **12** 65
- [101] Protheroe R J et al 1997 *Proc. of 25th ICRC, Durban* **8** 317
- [102] Aharonian F et al 1999 *Astron. Astrophys.* **349** 29
- [103] Giovannini G et al 1998 *Proc. 'BL Lac Phenomenon Conference', Turku* (ed. Leo Takalo)
- [104] Buckley J H et al. 1996 *Astrophys. J.* **472** L9
- [105] Kranich D et al. 1999 *Proc. of 26th ICRC, Salt Lake City* **3** 358
- [106] de Jager O C et al. 1999 *Proc. of 26th ICRC, Salt Lake City* **3** 346
- [107] Cui et al. 1998 *Proc. 'The Third William Fairbank Meeting on THE LENSE - THIRRING EFFECT', Pescara, Italy,* Electronic preprint astro-ph/9811023
- [108] *Proc. 'The Hubble Deep Field', ed M. Livio, STScI Symposium Series, May 1997*
- [109] Chounet L 1999 These proceedings
- [110] Pian E. et al. 1998 *Astrophys. J.* **492** L17
- [111] Samuelson F. et al. 1998 *Astrophys. J.* **501** L17
- [112] Djannati-Atai A et al. 1999 *subm. to Astron. Astrophys.* Electronic preprint astro-ph/9906060
- [113] Aharonian F et al 1999 *Astron. Astrophys.* **342** 69
- [114] Vassiliev V V 1999 *to appear in Astropart. Phys.* Electronic preprint astro-ph/9908088
- [115] Biller S D et al. 1998 *Phys. Rev. Lett.* **80** 2992
- [116] Primack J R et al 1999 *Astropart. Phys.* **11** 93
- [117] Malkan M A and Stecker F W 1999 *Astrophys. J.* **496** 13
- [118] Amelino-Camelia G et al. 1997 *Mod. Phys.* **A12** 607
- [119] Biller S D et al. 1999 *Phys. Rev. Lett.* **83** 2108
- [120] Magnussen N 1999 *Proc. of 26th ICRC, Salt Lake City* **4** 100
- [121] Waxman E and Bahcall J N 1997 *Phys. Rev. Lett.* **78** 2292
- [122] Gaisser T K, Halzen F, Stanev T 1995 *Phys. Rep.* **258** 3
- [123] Halzen F 1999 *Proc. of 26th ICRC, Salt Lake City* **2** 428
- [124] Porrata R 1997 *Proc. of 25th ICRC, Durban* **7** 9
- [125] Rhode W et al. 1996 *Astropart. Phys.* **4** 217
- [126] Andres E et al. 1999 *subm. to Astropart. Phys.* Electronic preprint 9906203
- [127] Spiering C 1999 *Proc. 8th Int. Workshop on Neutrino Telescopes, Venice, Italy*
- [128] Spiering C 1998 *Prog. Part. Nucl. Phys.* **40** 391
- [129] Balkanov V A et al. 1999 *Proc. Beyond the Desert99: Accelerator, Non-Accelerator and Space Approaches, Castle Ringberg, Tegernsee, Germany*
- [130] Mannheim K 1995 *Astropart. Phys.* **3** 295
- [131] Bertin V 1999 These proceedings